Live Load Distribution in Integral Composite Steel Bridges

SAMI W. TABSH and SHEHAB MOURAD

ABSTRACT

In recent years, there has been an increased interest in integral bridges for highway applications due to their inherent economy, serviceability, and strength. This study deals with the live load distribution of integral composite steel bridges near the abutments. Girder distribution factors for shear and bending moment in interior as well as in exterior beams are determined. A comparison between the response of integral bridges and their jointed counterpart is also included. Single and continuous spans are considered in the investigation. The applied loading is composed of several side-by-side HS20 trucks. Linearly elastic finite element analysis is used to analyze the three-dimensional bridge systems. The results of the study indicated that shear in the interior beams and the corresponding girder distribution factor are lower in integral bridges than in simply supported bridges. As the pile length to fixity increases, the shear and moment in the beams near the integral abutment decrease. Further, as the length of the wingwalls in integral bridges increases, the shear and moment in the interior beams increase.

INTRODUCTION

By definition, integral bridges are bridges with no joints between the superstructure and the abutments.[1] The superstructure of integral bridges can be constructed with composite steel or prestressed concrete girders. The abutments consist of an abutment wall, two wingwalls, and several supporting piles along a line under the abutment wall and at the free end of the wingwalls, as shown in Figure 1. The abutment walls and wingwalls are usually reinforced concrete members. The piles are made with either structural steel or precast concrete. Currently, some state departments of transportation in the United States impose certain restrictions on the geometry of integral bridges. For example, there is a limit on the total bridge length, skew angle, vertical grade, and horizontal alignment.

The increasing interest in jointless bridges is because experience has shown that joints in the deck are a continuing problem in existing bridges. The problem with joints is the need for continuing maintenance because of corrosion damage in the girders and underlying substructure, caused by leaking run-off water containing corrosive de-icing salts through the joints in the deck.[2] Integral bridges are usually economical due to the presence of fewer piles, elimination of bearings, lack of expansion joints and diaphragms at the abutments, and utilization of nonbattered piles. Other advantages of integral bridges include simplified construction procedures, increased redundancy, and improved seismic performance. Further, the lack of joints in integral bridges enhances their aesthetics.[3]

Most of the recently published research on integral bridges has been concerned with studying the thermal and creep effects,[4,5] and seismic behavior.[6,7] A literature search indicates that there are limited research studies on live load analysis of integral bridges. Further, there is no guidance in the current bridge design specifications on to how to compute the girder distribution factors for such bridges and whether the distribution factors for conventional bridges in the specification are valid or not for use with integral bridges.

INTEGRAL VERSUS JOINTED BRIDGES

There are many differences between integral bridges and their jointed counterparts. Abutments used with jointed bridges must resist embankment pressures by their own inherent

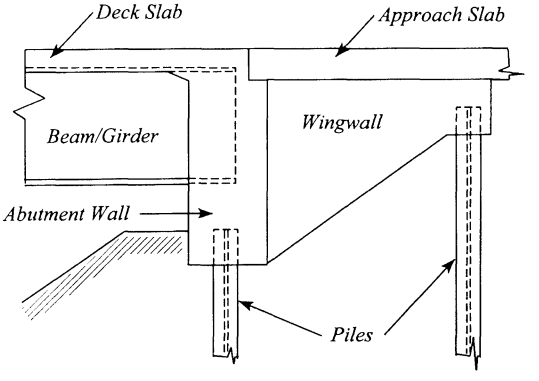

Fig. 1. Connection detail for a composite steel integral bridge.

Sami W. Tabsh is assistant professor, department of civil and environmental engineering, University of Houston, Houston, TX.

Shehab Mourad is assistant professor, department of civil engineering, Ain Shams University, Cairo, Egypt.

strength, whereas integral pile cap-type abutments resist embankment pressures by transferring the load to the superstructure, which acts as a column. This results in cost savings in integral bridges because they receive much of their longitudinal and lateral support from the embankments. In addition, the simple details in integral bridges result in rapid and economical construction. This is mainly because integral bridges do not require construction of bridge seats, separate backwalls, and end diaphragms or the furnishing of bearings and deck joints. Additionally fewer, non-battered piles are normally used with integral bridges. Also, integral bridges have high resistance to deicing chemical corrosion and deterioration because deck drainage cannot penetrate the bridge slab and adversely affect the bridge girders and substructure.

SCOPE

The scope of the study deals with the behavior of integral abutments supporting composite steel superstructures under the application of truck loads. Live load girder distribution factors for negative moment and shear near the abutments are considered. The investigation covers both interior and exterior girders. Bridges with single spans as well as with continuous spans are treated in the study. The loading consists of one or more side-by-side HS20 trucks, in accordance with the AASHTO's Load Factor Design provisions.[8] The linearly-elastic finite element method is used to analyze the three-dimensional bridge systems.

OBJECTIVES

There are three main objectives for this study that deals with integral bridges:

1. to compute live load girder distribution factors for moment as well as for shear near the integral abutments,
2. to evaluate the sensitivity of the girder distribution factors to changes in the superstructure geometry and continuity, pile spacing and stiffness, and wingwall length, and
3. to compare the results of the analysis of integral bridges with those obtained for conventional steel girder bridges supported on bearings.

MODELING OF THE SUPERSTRUCTURE

The bridges in this study are analyzed elastically using the finite element program ALGOR.[9] The reinforced concrete deck slab is modeled by three-node triangular and 4-node rectangular shell elements. These finite elements are located in the model at the mid-depth of the slab. The triangular elements are used in the vicinity of the applied concentrated wheel loads. The shell elements consider in-plane and out-of-plane deformations with five degrees-of-freedom at each node accounting for three translations and two rotations. The top and bottom flanges of the steel girders are modeled using space beam elements with six degrees of freedom at each of the two nodes. The beam elements with their properties are lumped at the centroid of the flanges. The steel webs of the bridge beams are modeled by four-node rectangular shell elements similar to those used in the concrete slab. The intermediate diaphragms are composed of cross frames made from steel angles and are modeled using space truss elements having three-displacement degrees of freedom at each node. Rigid beam elements are placed between the centroids of the top flange beam elements and the deck slab shell elements in order to satisfy the compatibility of the composite behavior and account for the thickness of the haunch and deck slab.

MODELING OF THE SUBSTRUCTURE

The reinforced concrete abutment walls and wingwalls are modeled by eight-node solid elasticity elements with three translational degrees-of-freedom at each node. The supporting steel H-piles are represented by two-node space beam elements spanning between the bottom of the abutment wall/wingwalls and the equivalent point of fixity of the piles inside the soil. The piles extend inside the abutment and wingwall a distance equal to 0.45-0.6 m, hence the connection at the top of the piles to the structure can be considered rigid. The equivalent point of fixity is determined based on the pile load-deflection relationships and is usually a function of the soil type, magnitude of the applied axial and lateral loads, presence and location of water table, and pile dimensions and stiffness. The approximate modeling of the piles by rigidly supported beams simplifies the analysis because it eliminates the need for a detailed modeling of the soil around the piles. Such an approximation is appropriate for structures subjected to gravity loads because the piles are normally installed in oversize, pre-augered holes for the top 3 to 6 m portion of the piles, with at least an equal embedment length into acceptable subsurface soils. A summary of the finite element model of a typical integral bridge is shown in Figure 2.

BRIDGES CONSIDERED

Four different composite steel bridges with integral abutments are considered in this study. The abutment walls for all

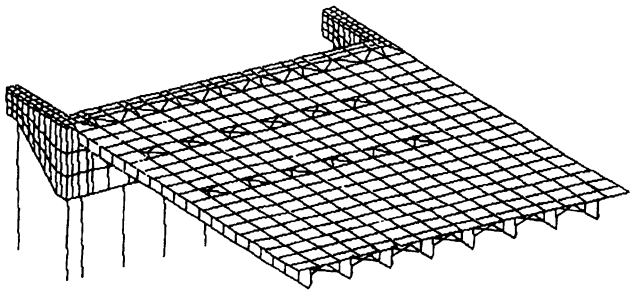

Fig. 2. Finite element modeling of a portion of an integral bridge.

the bridges are 14 m long, 0.75 m thick, and 2.75 m deep. Also, each wingwall is 3.5 m long, 0.50 m thick, with a nonprismatic depth varying between 1.0 m at the free end and 2.75 m near the abutment. Either eleven or twelve HP307×79 steel piles are used to support the bridge substructures of the four bridges at each abutment, including one pile under the free end of each wingwall. The length to the point of fixity of the piles is 3.0 m at the abutment wall and 4.75 m at the end of the wingwalls, as shown in Figure 3. The specified 28-day compressive strength of concrete in the deck slab and substructure is 28 MPa. The modulus of elasticity of the structural steel in the beams, intermediate cross frames, and piles is taken equal to 200 GPa. Detailed description for the four considered bridges is presented below.

Bridge 1 is a 3-lane composite steel I-beam bridge with a roadway width between the parapets equal to 13 m. The superstructure cross sections of the bridge is composed of a 0.22 m thick concrete slab on four W920×416 steel beams that are spaced at 3.5 m with 1.75 m overhangs, as shown in Figure 4. Bridge 1 has a single span with clear length between the abutment walls equal to 25 m. The thickness of the concrete haunch between the top steel flanges and the deck slab is equal to 20 mm. The width of the concrete parapets is 0.5 m. The cross-bracing consists of L89×89×12.5 angles at the third points, with no diaphragms at the abutments.

Bridge 2 is similar in all aspects to bridge 1 with the exception that the superstructure is two-span continuous with equal spans of 25 m each. In bridge 2, the cross sectional areas of the top and bottom flanges of the steel beams are doubled to account for increased flange dimensions in the negative-moment region, near the pier. The connection between the continuous superstructure and the pier is modelled by an external hinge at the bottom of each beam. The hinge connection does not permit translation in any direction, but allows rotation about any horizontal or vertical axis.

Bridge 3 is composed of a 0.20 m thick concrete slab on eight W920×271 steel beams that are spaced at 1.75 m with 0.875 m overhangs, as shown in Figure 5. It has a single span with clear length between the abutment walls equal to 25 m. The bridge width, parapet size, haunch thickness, and cross bracing dimensions are the same as in bridge 1.

Finally, bridge 4 has the same superstructure as for bridge 3, but is continuous with two equal spans of 25 m. The connection detail at the pier location is the same as in bridge 2.

Bridges 1–4 are also analyzed with the superstructures being simply supported on the abutments, with no restraint to the beam rotation. These cases are considered in order to compare the results of integral bridges with those obtained from conventionally supported bridges.

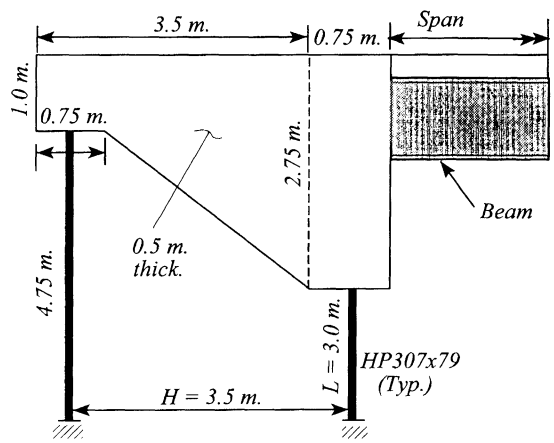

Fig. 3. Dimensions of wingwall and abutment.

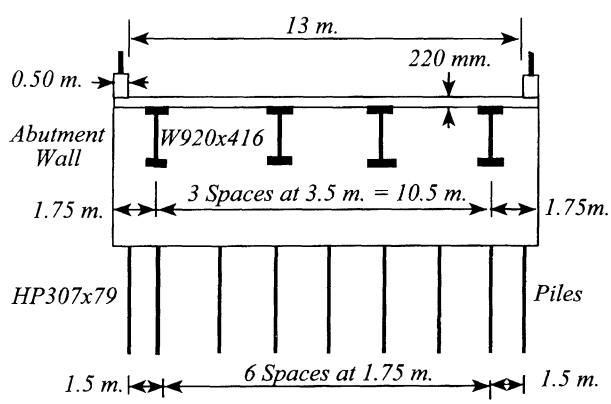

Fig. 4. Cross section of bridge 1 at the abutment.

RESULTS OF THE ANALYSIS

The four considered bridges are subjected to several side-by-side HS20 trucks placed inside 3.60 m lanes, in accordance with the AASHTO code.[8] The trucks are longitudinally positioned such that the live load reaction of the beams at the abutment location is maximized. The transverse position of

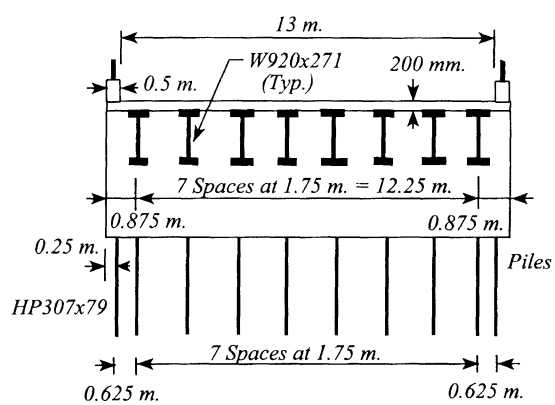

Fig. 5. Cross section of bridge 3 at the abutment.

the trucks is based upon maximizing the load on the interior beams. The minimum distance of a wheel from the inside edge of the parapet or between two side-by-side trucks is taken equal to 1.20 m. Both shear and bending moment in the composite steel beams near the integral abutments are investigated in the study.

Shear in the Beams

The shear stress and wheel load girder distribution factor for shear, GDF, for the interior and exterior beams near the abutment in the considered integral bridges are determined for a number of cases. In addition to the standard cases discussed earlier, each integral bridge is considered with different pile lengths, L, and wingwall lengths, H, where L and H are as defined in Figure 3. The GDF can be obtained as a function of the shear stress in the girder webs as follows:

$$GDF = \frac{2Nv_j}{\sum_{i=1}^{n} V_i} \quad (1)$$

where

v_j = shear stress in the web of the beam under consideration
v_i = shear stress in the web of beam i
n = number of beams
N = number of trucks on the bridge

The results of the analysis of integral bridges are compared with the corresponding results for bridges having simple supports at the abutment location. The finite element analysis of the simply supported bridges resulted in GDF values for shear in interior beams equal to 2.29 and 1.15 for bridge 1 and bridge 3, respectively. The corresponding GDF for the 2-span continuous bridges were very close to the single span bridges. For comparison purposes, the girder distribution factors for shear in interior girders due to axles near the abutment following the AASHTO's LFD code[8] are equal to 2.26 and 1.04 for bridge 1 (or bridge 2) and bridge 3 (or bridge 4), respectively. The corresponding girder distribution factors based on the AASHTO's LRFD code[10] are equal to 2.21 and 1.30, respectively.

Figures 6 and 7 show, respectively, the sensitivity of shear and GDF in the heavily loaded interior beams due to changes in the pile length. The results of the analysis of the integral bridges are presented in terms of the results of the corresponding simply supported bridges. Figure 6 indicates that the first interior beams in the considered integral bridges are subjected to about 20–25 percent less shear than in the corresponding beams in the simply supported bridges. Also, as the length of the piles in integral abutments increases, the shear stress decreases. Figure 7 shows that the shear in the superstructure near the abutment is more uniformly distributed among the beams in the integral bridges than in the simple supported ones. On average, the GDF for shear in integral bridges is about 10 percent less than in bridges supported on bearings.

The effect of the length of the wingwall on shear and GDF is shown in Figures 8 and 9, respectively. The findings indicate that both shear and GDF are lower in integral bridges than in simply supported bridges. Figures 8 and 9 show that as the wingwall length increases, the shear in the interior beam increases slightly. However, the increase in shear is accompanied by a slight decrease in the corresponding GDF.

A comparison between the shear behavior of interior and exterior beams is presented in Figure 10. The results of the analysis show that exterior beams behave the same as interior beams when the pile length and wingwall length change. However, although the magnitude of the shear in interior and exterior beams in integral bridges are smaller than those in simply supported bridges, the girder distribution factors for the exterior girders are about 0–15 percent larger in the integral bridges.

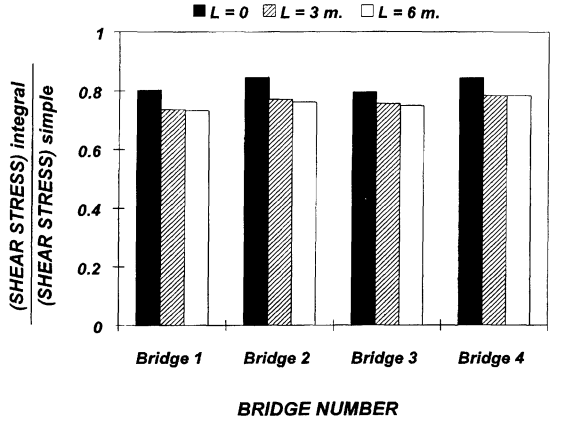

Fig. 6. Effect of pile length on shear stress in beams.

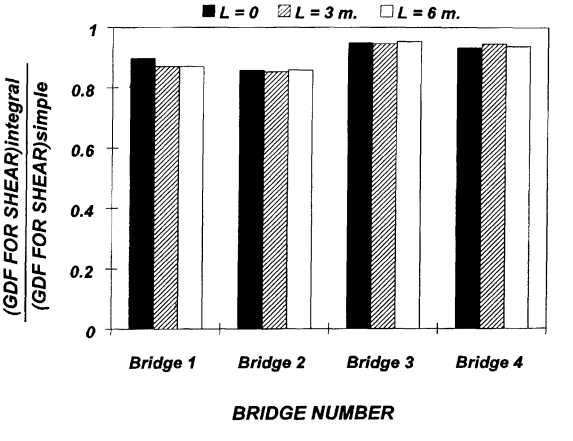

Fig. 7. Effect of pile length on girder distribution factor for shear.

Moment in the Beams

The flexural behavior of the steel beams near the integral abutments is studied in terms of the tensile stresses in the top flanges near the loaded abutment since under linearly elastic conditions the bending moment is proportional to the longitudinal stress in the beam. The relationship between the flexural stress and the wheel load girder distribution factor for moment, GDF, is given by:

$$GDF = \frac{2Nf_j}{\sum_{i=1}^{n} f_i} \tag{2}$$

where

f_j = extreme top flange stress of the beam under consideration
f_i = extreme top flange stress of beam i

and all other variables were defined earlier.

The sensitivity of the flexural stress and GDF for moment in the heavily loaded interior beams near the integral abutment due to changes in the pile length is shown in Figures 11 and 12, respectively. In general, Figure 11 indicates that as the length of piles increases, the flexural stress on the top of the considered interior beams decreases for both single and continuous span bridges. The corresponding girder distribution factor for bending moment in the interior beams is slightly affected by the change in the pile length to the point of fixity, as shown in Figure 12.

Figures 13 and 14 show the sensitivity of the bending moment and GDF for interior beams at the abutment location due to changes in the wingwall length. The results of the analysis indicate that the flexural stresses on top of the beams increase with an increase in wingwall length. This is accompanied by a decrease in the corresponding girder distribution factors, thus indicating that the live load distribution is more

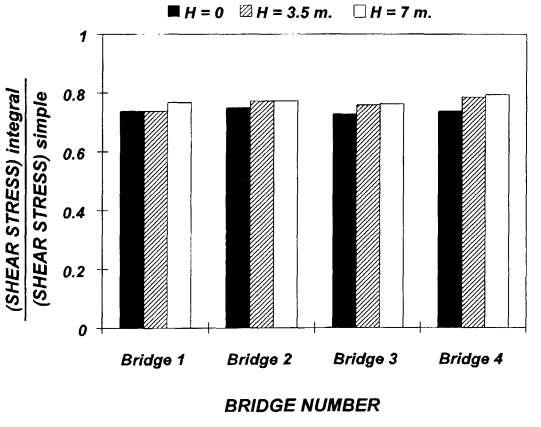

Fig. 8. Effect of wingwall length on shear stress in beams.

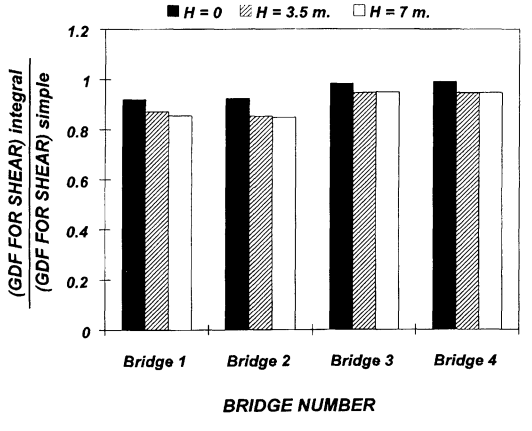

Fig. 9. Effect of wingwall length on girder distribution factor for shear.

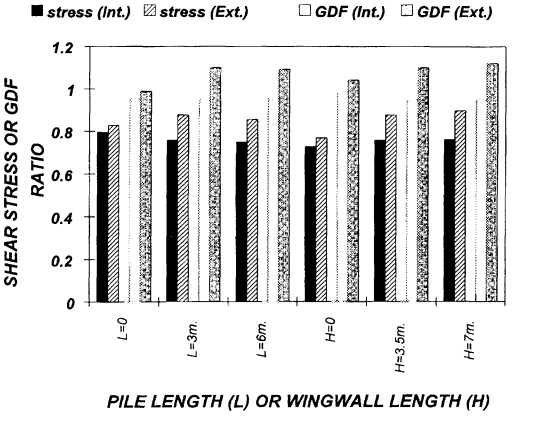

Fig. 10. Comparison between the shear behavior in interior and exterior beams.

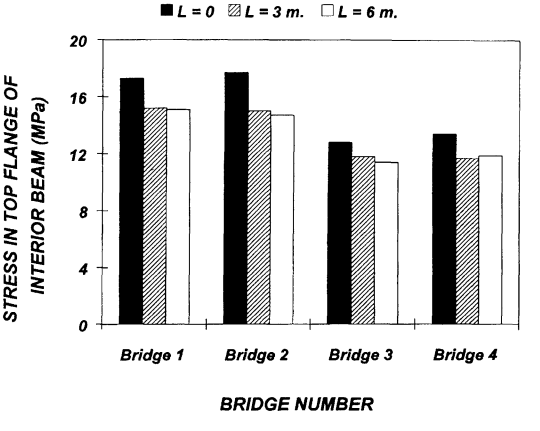

Fig. 11. Effect of pile length on flexural stress in beams.

uniform in integral bridges with long wingwalls than with short ones.

Figure 15 shows a comparison between the flexural stresses and girder distribution factors of exterior and interior beams. The findings indicate that exterior and interior beams behave similarly in flexure due to changes in the geometry of the integral bridge. Further, the stress on the top of the beam and the corresponding GDF for bending are slightly smaller in exterior beams than in interior beams for all cases except when the pile length or wingwall length are equal to zero. In the later cases, the stresses and GDF are about 5–10 percent larger in the exterior beams.

CONCLUSIONS

The results of this investigation lead to the following conclusions regarding the considered bridges:

1. In general, both shear in the interior beams and the corresponding girder distribution factor are lower in integral bridges than in simply supported bridges. However, the girder distribution factor for shear in exterior girders in integral bridges is slightly higher in integral bridges than in corresponding bridges supported on bearings.
2. As the length to fixity of the supporting piles increases, the shear and moment in the interior beams near the integral abutment decrease.
3. As the length of the wingwalls in integral bridges increases, the shear and moment in the interior beams increase. However, the increase in shear and moment is accompanied by a decrease in the corresponding girder distribution factors.

REFERENCES

1. Burke, M. P., Jr., "Bridge Approach Pavements, Integral Bridges, and Cycle Control Joints," *Transportation Re-*

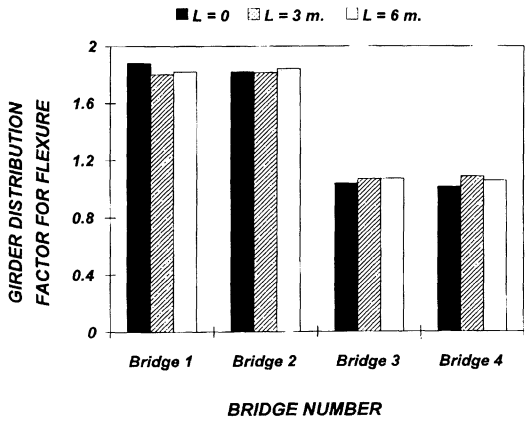

Fig. 12. Effect of pile length on girder distribution factor for flexure.

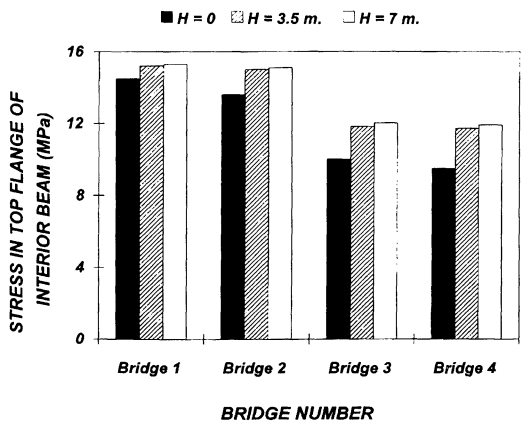

Fig. 13. Effect of wingwall length on flexural stress in beams.

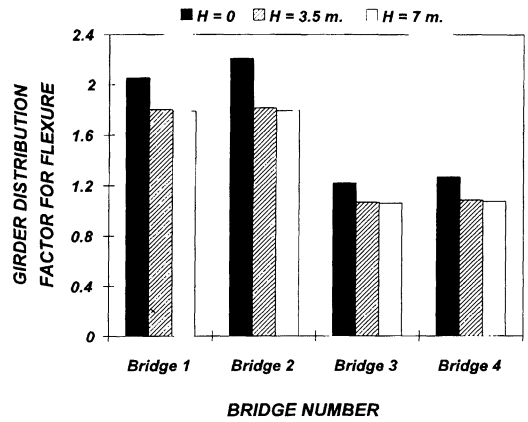

Fig. 14. Effect of wingwall length on girder distribution factor for flexure.

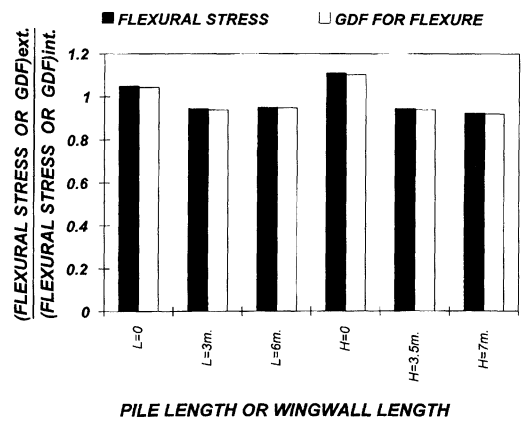

Fig. 15. Comparison between the flexural behavior in interior and exterior beams.

search Record, No. 1113, TRB, National Research Council, Washington, D.C., 1987, pp. 54–65.
2. Loveall, C. L., "Jointless Bridge Decks," ASCE *Civil Engineering*, November, 1985.
3. Burke, M. P., Jr., "Integral Bridges: Attributes and Limitations," *Transportation Research Record, No. 1393, TRB*, National Research Council, Washington, D.C., 1993, pp. 1–8.
4. Siros, D., and Spyrakos, C., "Creep Analysis of Hybrid Integral Bridges," *Transportation Research Record, No. 1476, TRB*, National Research Council, Washington, D.C., 1995, pp. 147–154.
5. Siros, D., and Spyrakos, C., "A study of Jointless Bridge Behavior," ASCE *Proceedings of XII Structures Congress*, Atlanta, 1994, pp. 485–489.
6. Wilson, J. C., "Stiffness of Non-Skewed Monolithic Bridge Abutments For Seismic Analysis," *Earthquake Engineering and Structural Dynamics*, Vol. 16, January, 1988, pp. 867–883.
7. Cook, T. L., Burdette, E. G., Graves, R. L., Goodpasture, D. W., and Deatherage, J. H., "Effect of Varying Foundation Stiffness on Seismically Induced Loads in Bridge Bents: A Sensitivity Study," *Transportation Research Record, No. 1476, TRB*, National Research Council, Washington, D.C., 1995, pp. 84–97.
8. American Association of State Highway and Transportation Officials, *Standard Specifications for Highway Bridges*, Sixteenth Edition, Washington, D.C., 1996, 677 pp.
9. ALGOR, *Reference Manual*, Pittsburgh, 1994.
10. American Association of State Highway and Transportation Officials, *LRFD Bridge Design Specifications—SI Units*, First Edition, Washington, D.C., 1994.